

## Polymer mixtures in confined geometries: Model systems to explore phase transitions

K BINDER<sup>1</sup>, M MÜLLER<sup>1</sup>, A CAVALLO<sup>1</sup> and E V ALBANO<sup>2</sup>

<sup>1</sup>Institut für Physik, Johannes Gutenberg-Universität, D-55099 Mainz,  
Staudinger Weg 7, Germany

<sup>2</sup>INIFTA, Universidad Nacional de La Plata, C.C. 16 Suc. 4, 1900 La Plata, Argentina  
E-mail: kurt.binder@uni-mainz.de

**Abstract.** While binary (A,B) symmetric polymer mixtures in  $d = 3$  dimensions have an unmixing critical point that belongs to the  $3d$  Ising universality class and crosses over to mean field behavior for very long chains, the critical behavior of mixtures confined into thin film geometry falls in the  $2d$  Ising class irrespective of chain length. The critical temperature always scales linearly with chain length, except for strictly two-dimensional chains confined to a plane, for which  $T_c \propto N^{5/8}$  (this unusual exponent describes the fractal contact line between segregated chains in dense melts in two spatial dimensions,  $d = 2$ ). When the walls of the thin film are not neutral, but preferentially attract one species, complex phase diagrams occur due to the interplay between capillary condensation and wetting phenomena. For ‘competing walls’ (one wall prefers A, the other prefers B) particularly interesting interface localization–delocalization transitions occur, while analogous phenomena in wedges are related to the ‘filling transition’.

**Keywords.** Polymers; phase separation; wetting; Monte Carlo simulation; finite size scaling.

**PACS Nos** 61.41.+e; 64.75.+g; 68.45.Gd; 83.80.Es

### 1. Introduction

Symmetric binary (A,B) polymer blends are model systems for the theoretical and experimental study of phase separation, since the chain length  $N_A = N_B = N$  can (in principle) be varied over a wide range, and variation of this control parameter changes the entropy but does not affect the enthalpic forces between the monomers. In addition, the large size of the polymer coils (measured by the gyration radius  $R_g \approx a\sqrt{N/6}$  where  $a$  is the size of an effective monomer) allows us to apply additional experimental techniques; e.g., nuclear reaction analysis allows us to measure the concentration profile across unmixed polymer films [1,2].

The enthalpic forces between the atoms of the two species in a polymer mixture are similar to a mixture of small molecules while the entropy of mixing is down by a factor of  $N$  [3–5]. Therefore the critical temperature  $T_c$  of the unmixing transition

scales linear with chain length,  $k_B T_c \equiv z_c N \varepsilon$ , where (for a lattice model such as the bond fluctuation model [6] on the simple cubic lattice [7])  $\varepsilon$  is the strength of the (square-well) potential between the effective monomers and  $z_c$  the effective coordination number [8–10]. This linear scaling has been nicely confirmed both by computer simulations in  $d = 3$  dimensions [8,9,11,12] and by experiment [13].

For  $N \rightarrow \infty$  even the prefactor in the relation between  $T_c$  and  $N$  is accurate [8–10], while for finite  $N$  there are  $1/\sqrt{N}$ -type corrections [8,9] due to the ‘correlation hole effect’ [4] and concentration fluctuations neglected in the mean field theories. The fact that the Flory–Huggins mean field theory [3–5] becomes quantitatively accurate is due to the strong interpenetration of the Gaussian polymer coils: since within the volume ( $V \approx 4\pi R_g^3/3$ ) that one coil occupies the density of its own monomers  $\rho$  scales as  $\rho = N/V \propto N^{-1/2}$ , each chain interacts with  $N^{1/2}$  other chains in a dense melt. The situation is similar to an Ising model with a large range,  $R$ , of the interaction [14], and as in the latter model, one can observe an interesting cross-over in the critical behavior from mean field-like (if the reduced distance  $|t|$  from  $T_c$ ,  $t = 1 - T/T_c$ , exceeds by far the ‘Ginzburg number’  $Gi$ ,  $|t| \gg Gi$  [14,15]) to the  $3d$  Ising universality class [17], for  $|t| \ll Gi$ . Note that  $Gi \propto 1/N$  for binary polymer mixtures [16]. The cross-over scaling [14] has been tested successfully for polymer mixtures both in simulations [12] and in experiment [18].

However, the situation changes completely when we consider polymer blends confined in thin films, mean field theory loses its validity, critical behavior of the  $2d$  Ising universality class and interesting cross-over behavior occur [10,19,20]. This problem is considered in the following sections.

## 2. Strictly two-dimensional polymer blends

Since no two monomers can sit on top of the other, in  $d = 2$  chains cannot cross, and hence in dense melts in  $d = 2$  chains are well-segregated from each other. While in the dilute case one has  $R_g \propto N^\nu$  and  $\nu = 3/4$  in  $d = 2$  [4], in a dense melt one still has  $R_g \propto N^{1/2}$ , but unlike the case of  $d = 3$  only monomers at the outer contour of a coil can have contacts with monomers of the other chains, while (for short-range interactions) monomers in the interior of a coil have only intrachain contacts, which do not contribute to phase separation, and no interchain contacts. While in  $d = 3$  each chain has  $z_c N$  interchain contacts and for  $N \rightarrow \infty$ ,  $z_c$  tends to a finite constant, we expect that  $z_c \propto N^{-x}$  in two dimensions, where  $x$  is an exponent that is discussed below, and hence we expect that  $T_c \propto N^{1-x}$ . If the coils in  $d = 2$  were simply compact disk-like objects, we would expect that the outer contour scales like  $R \propto N^{1/2}$  and hence also [10]  $x = 1/2$ . However, this picture is too simple, and actually one can show that the outer contour of a chain in a dense melt is a fractal object [21] of length  $\ell \propto N^{5/8}$ , and hence  $x = 3/8$ . This yields the prediction  $T_c \propto N^{5/8}$  in  $d = 2$ .

In order to study this problem numerically, the bond fluctuation model on the simple cubic lattice in the  $L \times L \times D$  geometry is considered. In this model, each effective monomer blocks all the eight sites of an elementary cube, and these monomers are connected by bond vectors  $\vec{b}$  which may have the lengths  $b = 2, \sqrt{5}, \sqrt{6}, 3$  and  $\sqrt{10}$ , respectively. We measure all lengths in units of the lattice spacing. The

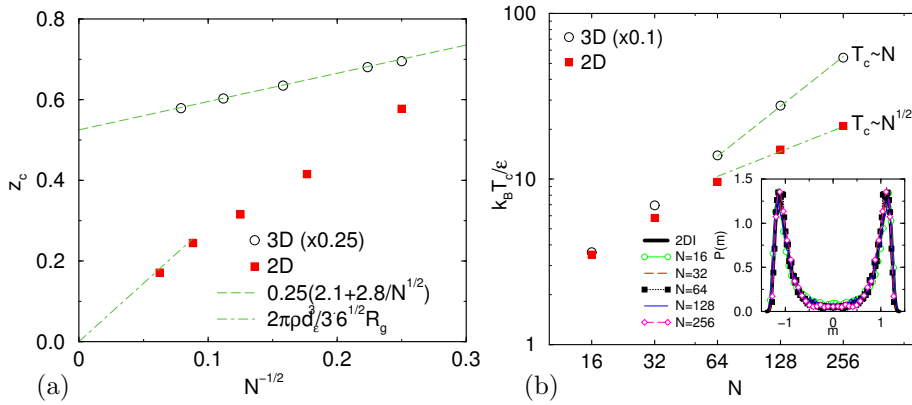


**Figure 1.** (a) Effective coordination number  $z_c$  plotted vs.  $N^{-1/2}$ . The dash-dotted line shows the approximation [10] appropriate for segregated compact coils,  $z_c = 2\pi\rho d_\epsilon^3 / (3\sqrt{6}R_g)$ . However, the best fit to all data points yields an effective power law [10]  $z_c \propto N^{-0.43}$ . For  $d = 3$  [8]  $z_c = 2.1 + 2.8/\sqrt{N}$ . (b) Log-log plot of the critical temperature  $k_B T_c / \epsilon$  plotted vs. chain length  $N$ . The straight lines indicate the power laws  $T_c \propto N$  and  $T_c \propto N^{1/2}$ , respectively. However, the best fit to all 2d data yields an effective power law  $T_c \propto N^{0.65}$  [10]. The inset presents the mapping of the normalized order parameter distribution at criticality onto the universal curve which characterizes the 2d Ising universality class [24]. From Cavallo *et al* [10].

chain length  $N$  is varied from 16 to 256, and the linear dimensions chosen are  $L = 256$  for  $N \leq 128$  and  $L = 512$  for  $N = 256$ , while  $D$  has the minimum value,  $D = 2$ . So the film is strictly two-dimensional, choosing hard impenetrable but neutral walls at  $z = 0$  and  $z = D + 1 = 3$ , while in  $x$  and  $y$  directions periodic boundary conditions are used. We choose a volume fraction  $\rho = 0.5$  of occupied sites, as in the case  $d = 3$  [7–9,11,12]. The number of chains is then  $\rho L^2 / 4N$ . As interaction between monomers, we use the most symmetric square well potential  $\varepsilon_{AA} = \varepsilon_{BB} = -\varepsilon_{AB} = -\varepsilon$  of range  $d_\varepsilon = \sqrt{5}$  as in previous work in  $d = 3$ . For planar configurations, this choice comprises 12 lattice sites instead of 54 as in  $d = 3$ .

Monte Carlo simulations were carried out [10,20] in the semi-grandcanonical ensemble [8,9,11,12], i.e., both  $\rho$  and  $T$  are fixed, as well as the chemical potential difference  $\Delta\mu$  between the two species. Chain configurations were updated by the ‘random hopping’ and ‘slithering snake’ algorithms [22], while the relative concentration of A chains, which constitutes the order parameter of the unmixing transitions, is relaxed by randomly attempted interchanges of A and B labels at fixed polymer conformation [5,9,10,22]. Initial configurations were generated by the ‘configurational bias’ method [23].

Figure 1a shows a plot of the effective coordination number  $z_c$  vs.  $N^{-1/2}$ , defining  $z_c$  from the intermolecular pair correlation function  $g(\vec{r})$  via  $z_c = (\rho/4) \int_{r \leq d_\varepsilon} d^2\vec{r} g(\vec{r})$ . The best fit to the data yields [10]  $z_c \propto N^{-0.43}$ , intermediate between the geometric estimate [10]  $z_c \propto N^{-1/2}$  and the prediction [21]  $z_c \propto N^{-3/8} = N^{-0.375}$ . Figure 1b shows the results for the critical temperature.

While in  $d = 3$  the asymptotic linear scaling  $T_c \propto N$  is clearly seen, for  $d = 2$  a weaker increase of  $T_c$  with chain length occurs. The best fit quoted in [10],  $T_c \propto N^{0.65}$ , is rather close to the prediction [21]  $T_c \propto N^{5/8} = N^{0.625}$ . It is also interesting to note that the critical behavior (tested, e.g., via the universal order parameter distribution  $P(m)$  at criticality [24]) is always nicely compatible with the  $2d$  Ising class, no cross-over to mean field behavior occurs for which  $\log P(m) \propto -m^4$ . This is easily understood from the Ginzburg criterion [12,14,15]: the Ginzburg number  $Gi$  depends on the dimensionality  $d$ , i.e.,  $Gi \propto [N/(\rho R_g^d)]^{2/(4-d)}$ , which yields  $Gi \propto 1/N$  in  $d = 3$  and  $Gi \propto N^0 = \text{const.}$  in  $d = 2$ . This must be so because the number of chains a reference chain in  $d = 2$  interacts with becomes independent of its length. As a result we find that in  $d = 2$  mean field theory for polymer mixtures and related approximations (like the ‘random phase approximation’ [4,5]) fail qualitatively.

### 3. Cross-over between $d = 2$ and $d = 3$ in films with neutral walls

Experimentally, a strictly two-dimensional polymer blend would be difficult to prepare; it is much easier to prepare nanoscopically thin polymer films on substrates, choosing molecular weights and film thicknesses such that  $R_g \gg D$ . In the opposite limit,  $R_g \ll D$ , the two neutral walls have only a weak effect on  $T_c$ , but for any finite value of  $D$  the critical behavior very close to the film falls in the  $2d$  Ising class, since only in  $x, y$  directions can the correlation length grow to infinity.

Figure 2a shows now the analog of figure 1a but for film thicknesses  $2 \leq D \leq 19$ . It is clearly seen that already for  $D = 4$  one obtains a non-zero  $z_c(N \rightarrow \infty)$ , although  $z_c$  is much depressed in comparison with the bulk behavior. Only when the film thickness is smaller than the excluded volume screening length,  $D < \xi_{ev}$ , we can expect that for large  $N$  no other chains interact with the interior monomers of the quasi-two-dimensional coil, and  $z_c(N \rightarrow \infty) \rightarrow 0$ , recovering the behavior of the previous section. For dense melts,  $\xi_{ev}$  is comparable to the monomer size, and hence this regime is hardly detected here. When  $\xi_{ev} \ll D \ll R_g$ , each monomer of a considered chain has some neighbors from other chains, and hence  $z_c(N \rightarrow \infty)$  is non-zero. Note, however, that a chain takes a volume of order  $V = \pi R_g^2 D$  and hence the density  $\rho = N/V$  of monomers of that chain in this volume remains non-zero for  $N \rightarrow \infty$  (remember  $R_g^2 \propto N$  here). Hence each chain interacts only with a finite number of other chains in the thin film, when  $N \rightarrow \infty$ , in contrast to the bulk, where the number of other chains in the same volume increases like  $N^{1/2}$ . As a consequence, in thin films the ratio  $k_B T_c / (\varepsilon N z_c)$  does not converge to its mean field limit ( $k_B T_c / \varepsilon N z_c = 1$ ) for  $N \rightarrow \infty$ , unlike the bulk (see figure 2b). The decrease of  $z_c$  and the decrease of this ratio together imply that in the thin film geometry the compatibility of polymers is dramatically enhanced in comparison to the bulk (e.g., for  $D = 7$ ,  $N = 256$   $T_c$  is reduced by almost a factor 2.4).

Although for  $D > \xi_{ev}$  we have a scaling  $T_c \propto N$  as predicted by the Flory–Huggins mean field theory, there is no mean field critical behavior even if  $N \rightarrow \infty$ , the behavior stays  $2d$  Ising-like [19,20]. However, for rather thick films ( $D > R_g$ ), an interesting cross-over behavior is predicted [19]. Remember that in the bulk the

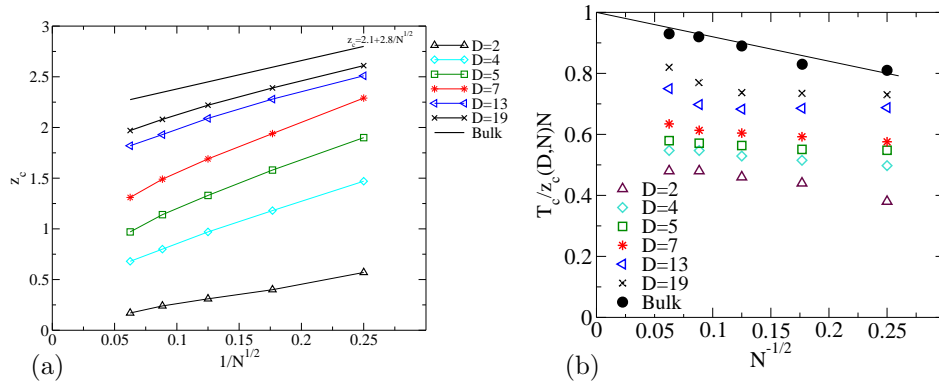


**Figure 2.** (a) Effective coordination number  $z_c$  plotted vs.  $N^{-1/2}$  for films with neutral walls, choosing film thickness  $2 \leq D \leq 19$ . The bulk behavior is included for comparison. (b) Normalized critical temperature  $k_B T_c / (\varepsilon N z_c)$  plotted vs.  $N^{-1/2}$  for  $2 \leq D \leq 19$ . The bulk behavior is included for comparison. From Cavallo *et al* [20].

cross-over between mean field and 3d Ising behavior occurs for  $|t|/G_i$  of order unity, i.e., a correlation length  $\xi$  of order  $\xi_{\text{cross}} = R_g \sqrt{N}$ . If  $R_g < D < \xi_{\text{cross}}$ , one observes cross-over from mean field critical behavior to 2d Ising behavior when  $\xi$  becomes of order  $D$ , i.e., ( $\xi_{\text{MF}} \propto R_g |t|^{-1/2}$ ) for  $|t| = (R_g/D)^2$ . If  $D > \xi_{\text{cross}}$ , however, one first crosses over from mean field to 3d Ising behavior at  $\xi = \xi_{\text{cross}}$  (like in the bulk) and only when  $\xi = D$  one observes a cross-over from 3d Ising behavior to 2d Ising behavior. While these multiple cross-overs have been analysed phenomenologically [19], in practical cases one often cannot resolve these limiting behaviors, but rather observes ‘effective exponents’ intermediate between the 2d and 3d Ising behavior [19].

#### 4. Thin films with both the walls preferentially attract the same species

In practice the assumption of a polymer mixture confined between ‘neutral’ walls (no preferential attraction of one of the species) clearly will be an idealization, and it is of interest to consider the case that both walls preferentially attract, say, species A. When the temperature is decreased below the bulk unmixing critical temperature, A-rich layers gradually form at the walls. At low enough temperatures then a transition occurs to a state with laterally segregated phases (see figure 3) [25]. While in the bulk the critical composition of a symmetric (A,B) mixture occurs for  $\phi^{\text{crit}} = 1/2$  by symmetry, in the thin film it is shifted to the A-rich side (as shown in figure 4a) [26]. Similarly, while in the bulk phase coexistence occurs for a chemical potential difference  $\Delta\mu = 0$ , in the thin film it occurs along a (non-trivial) curve  $\Delta\mu_{\text{coex}}(T) < 0$  (see figure 4b). This is the analog of ‘capillary condensation’ of undersaturated gases in slit pores for binary mixtures. The shape of the coexistence curves near the critical point reflects the corresponding order parameter exponent  $\beta$ , namely  $|\phi_{\text{coex}} - \phi_{\text{crit}}| \propto (1 - T/T_c)^\beta$ , with  $\beta \approx 0.325$  [14] (bulk: 3d Ising

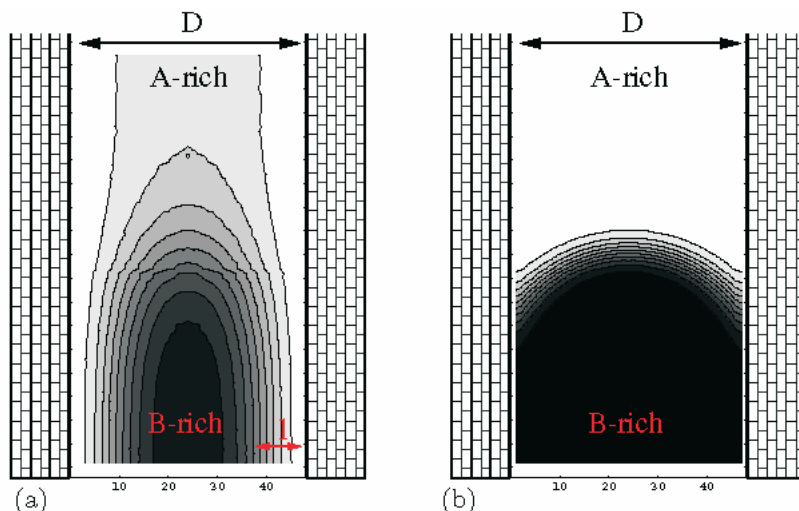


**Figure 3.** Monte Carlo results for the composition profiles of the interface between two coexisting phases in a thin film with symmetric surface interactions, for chain length  $N = 32$  and film thickness  $D = 48$ . A-rich regions are shaded light, B-rich regions are shaded dark, and contours of constant relative concentration  $\phi = \rho_A/\rho$  of A  $\phi = 0.9, 0.8, \dots, 0.1$  (from the walls towards the film interior in the left part) are shown; (a) corresponds to a temperature above the wetting transition temperature  $T_{\text{wet}}$  of a semi-infinite mixture, namely  $T \approx 3.5T_{\text{wet}}$ : there are A-enrichment layers in the B-rich region, and the AB interface does not approach the wall; (b) corresponds to a temperature below  $T_{\text{wet}}$ , namely  $T = 0.89T_{\text{wet}}$ . There is only a negligibly small surface enrichment of A in the B-rich phase, and the AB interface makes a finite angle with the wall (for  $D \rightarrow \infty$  this would be the contact angle). From Müller and Binder [25].

universality class) and  $\beta = 1/8$  [17] (thin film:  $2d$  Ising universality class), respectively. While in the semi-infinite system the model exhibits first-order wetting [25] and a prewetting line [27], the only remnant of these transitions in the thin symmetric film with  $D = 48$  is a ‘bulge’ in the coexistence curve near  $k_B T/\varepsilon \approx 20$ . Finally, we mention that for this model rather direct evidence for the renormalization of the effective interface potential by capillary wave fluctuations could be obtained [25,26].

### 5. Thin films with competing walls: Interface localization–delocalization transitions

In this section we consider the situation where the left wall attracts the A-component of the mixture with the same strength as the right wall attracts the B-component. The phase diagram for this situation for  $D = 48$  was already included in figure 4: the transition that occurs in the bulk for  $k_B T/\varepsilon = 69.3$  is rounded

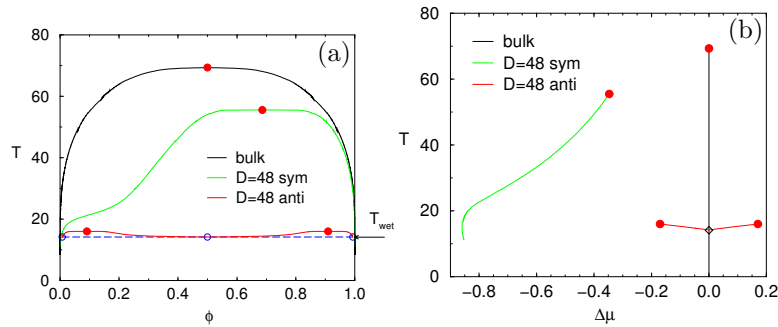


**Figure 4.** (a) Phase diagram of a binary polymer blend (A,B) described by the bond fluctuation model for  $N_A = N_B = N = 32$ . The upper curve shows the coexistence curve in the infinite system, ending in a critical point at  $\phi_{\text{crit}} = 1/2$  and  $k_B T_c / \varepsilon = 69.3$ . The middle one (broken curve) corresponds to a thin film of thickness  $D = 48$  and symmetric boundary fields  $\varepsilon_w = 0.16$ , which both ‘prefer’ species A. The arrow marks the location of the wetting transition ( $k_B T_{\text{wet}} / \varepsilon = 14.1$  [25]). The lower curve also corresponds to a thin film of thickness  $D = 48$ , but with ‘antisymmetric surfaces’ (see §5). There occurs a triple point at  $\phi_{\text{trip}} = 1/2$ ,  $T_{\text{trip}} \approx T_{\text{wet}}$ , and two critical points at  $T_c \approx 16$ ,  $\phi_{\text{crit}}^{(1)} \approx 0.09$  and  $\phi_{\text{crit}}^{(2)} \approx 1 - \phi_{\text{crit}}^{(1)}$ , respectively. (b) Coexistence curves in the  $(T, \Delta\mu)$  plane, for the same cases as in part (a). Circles mark critical points, and the diamond marks the location of  $T_{\text{wet}}$  (and  $T_{\text{trip}}$ ). From Müller and Binder [26].

off, since an interface between an A-rich domain at the left wall and a B-rich domain at the right wall forms gradually as  $T$  is lowered through  $T_c$ , from the corresponding enrichment layers that are already present above  $T_c$  [28]. For  $D \rightarrow \infty$  the unmixing transitions starting at  $T_c(D)$  turn into the prewetting transitions, while the transition at  $\Delta\mu = 0$ ,  $T_{\text{trip}}(D)$  becomes the wetting transition [28,29]. While with Monte Carlo methods only films with  $D \leq 48$  layers could be studied, the self-consistent field (SCF) method has allowed to study much thicker films and hence substantiate the above statements. However, the SCF method near critical points always yields mean field behavior only ( $\beta = 1/2$ ) and also does not include capillary wave-type effects.

A particularly interesting phenomenon occurs for antisymmetric films which are sufficiently thin, i.e., the two critical points in figure 4 and the triple point merge at a special, tricritical film thickness  $D_{\text{tri}}$ , and one finds a tricritical interface localization–delocalization transition [26,29]. For  $D < D_{\text{tri}}$ , the interface localization–delocalization transition is of second order, as studied for the simple Ising model [30,31]. A detailed analysis of the various cross-overs that occur near this tricritical point in the mean field description and beyond has been given [26] and tested by Monte Carlo methods [26]. Unfortunately, in real systems one can never expect perfect antisymmetry between the surface fields of the two walls, and then a tricritical point is no longer expected: rather one moves from a phase diagram with two (not symmetric) critical points and a triple point to a phase diagram with a single critical point (when the other critical point

and the triple point merge). This pattern of behavior has been demonstrated by SCF methods also [32]. However, in the weakly asymmetric case when the two walls prefer different phases with unequal strength one can still expect to see for  $T_{\text{wet}} < T < T_c$  the ‘soft mode phase’ with a strongly fluctuating interface unbound from the walls [33]. Indeed, a signature of such a phase, namely an anomalous dependence of the average interfacial width on film thickness [34], has been detected in experiments on polymer interfacial mixtures confined in a thin film geometry [2].

Very recently, these theoretical studies have been extended to polymer mixtures confined to an antisymmetric double wedge geometry [35]. An anomalous interface localization–delocalization transition, that occurs when the  $L \times L$  cross-section of the wedge diverges at fixed generalized aspect ratio  $L^3/L_y = \text{const.}$  ( $L_y$  being the linear dimension for the direction along the wedge) is observed. It has first been seen for the Ising model [36] and related to the wedge filling transition discussed by Parry *et al* [37] and is characterized by a very unusual set of critical exponents ( $\beta = 0, \gamma = 5/4, \nu_{\perp} = 1/4, \nu = 3/4$ ).

In conclusion, simulations and various theoretical calculations have unraveled an incredible wealth of phase transitions and critical phenomena for polymer mixtures in confined geometry. It is hoped that this work will stimulate more experimental efforts along these lines.

## Acknowledgements

MM thanks the Deutsche Forschungsgemeinschaft (DFG) for a Heisenbergstipend, and AC thanks the Max Planck Institute for Polymer Research, Mainz, for a Max Planck fellowship. Further financial support was provided by the DFG under grant Bi 314/17 and by the DAAD/PROALAR 2000. Generous access to supercomputers at the NIC Jülich, the HLRS Stuttgart, and the computing center of the University of Mainz is gratefully acknowledged.

## References

- [1] A Budkowski, *Adv. Polym. Sci.* **148**, 1 (1999)
- [2] T Kerle, J Klein and K Binder, *Eur. Phys. J.* **B7**, 401 (1999)
- [3] P J Flory, *Principles of polymer chemistry* (Cornell University Press, New York, 1953)
- [4] P G de Gennes, *Scaling concepts in polymer physics* (Cornell University Press, New York, 1979)
- [5] K Binder, *Adv. Polym. Sci.* **112**, 181 (1994)
- [6] I Carmesin and K Kremer, *Macromolecules* **21**, 2819 (1988)
- [7] H-P Deutsch and K Binder, *J. Chem. Phys.* **94**, 2294 (1991)
- [8] M Müller and K Binder, *Macromolecules* **28**, 1825 (1995)
- [9] M Müller, *Macromol. Theory. Simul.* **8**, 343 (1999)
- [10] A Cavallo, M Müller and K Binder, *Europhys. Lett.* **61**, 214 (2003)
- [11] H-P Deutsch and K Binder, *Europhys. Lett.* **17**, 691 (1991)
- [12] H-P Deutsch and K Binder, *J. Phys. France II* **3**, 1049 (1993)

- [13] M D Gehlsen, J H Rosedale, F S Bates, G D Wignall and K Almdal, *Phys. Rev. Lett.* **68**, 2452 (1992)
- [14] K Binder and E Luijten, *Phys. Rep.* **344**, 179 (2001)
- [15] V L Ginzburg, *Sov. Phys. Solid State* **1**, 1824 (1960)
- [16] P G de Gennes, *J. Phys. (Paris) Lett.* **38**, L441 (1977)  
J-F Joanny, *J. Phys.* **A11**, L117 (1978)  
K Binder, *Phys. Rev.* **A29**, 341 (1984)
- [17] M E Fisher, *Rev. Mod. Phys.* **46**, 587 (1974)
- [18] D Schwahn, G Meier, K Mortensen and S Janssen, *J. Phys. France II* **4**, 837 (1994)
- [19] Y Rouault, B Dünweg, J Baschnagel and K Binder, *J. Stat. Phys.* **80**, 1009 (1995)
- [20] A Cavallo, M Müller and K Binder, in preparation
- [21] A N Semenov and A Johner, *Euro. Phys. J.* **E12**, 469 (2003)
- [22] K Binder (ed.), *Monte Carlo and molecular dynamics simulations in polymer science* (Oxford Univ. Press, New York, 1995)
- [23] D Frenkel and B Smit, *Understanding molecular simulation: From algorithms to applications* (Academic Press, San Diego, 1996)
- [24] A D Bruce and N B Wilding, *Phys. Rev. Lett.* **68**, 193 (1992)
- [25] M Müller and K Binder, *Macromolecules* **31**, 8323 (1998)
- [26] M Müller and K Binder, *Phys. Rev.* **E63**, 021602 (2001)
- [27] M Müller and L G MacDowell, *Macromolecules* **33**, 3902 (2000)
- [28] K Binder, M Müller and E V Albano, *Phys. Chem. Chem. Phys.* **3**, 1160 (2001)
- [29] M Müller, E V Albano and K Binder, *Phys. Rev.* **E62**, 5281 (2000); *Int. J. Mod. Phys.* **B15**, 1867 (2001)
- [30] K Binder, D P Landau and A M Ferrenberg, *Phys. Rev.* **E51**, 2823 (1995)
- [31] K Binder, R Evans, D P Landau and A M Ferrenberg, *Phys. Rev.* **E53**, 5023 (1996)
- [32] M Müller, K Binder and E V Albano, *Europhys. Lett.* **49**, 724 (2000)
- [33] A O Parry and R Evans, *Physica* **A181**, 250 (1992)
- [34] A Werner, F Schmid, M Müller and K Binder, *J. Chem. Phys.* **107**, 8175 (1997)
- [35] M Müller and K Binder, *J. Phys. Condens. Matter* **17**, S333 (2005)
- [36] A Milchev, M Müller, K Binder and D P Landau, *Phys. Rev. Lett.* **90**, 13160 (2003); *Phys. Rev.* **E68**, 031601 (2003)
- [37] A O Parry, C Rascon and A J Wood, *Phys. Rev. Lett.* **83**, 5535 (1999)